Am J Cancer Res 2022;12(7):3014-3033
www.ajcr.us /ISSN:2156-6976/ajcr0142736

Original Article

Nuclear interaction of Arp2/3 complex and BRAF^{V600E} promotes aggressive behavior and vemurafenib resistance of thyroid cancer

Mourad Zerfaoui[1], Koji Tsumagari[1], Eman Toraih[1], Youssef Errami[1], Emmanuelle Ruiz[1], Mohammed Sohail M Elaasar[1], Moroz Krzysztof[2], Andrew B Sholl[3], Sameh Magdeldin[4,5], Mohamed Soudy[4], Zakaria Y Abd Elmageed[1,6], A Hamid Boulares[7*], Emad Kandil[1*]

Departments of [1]Surgery, [2]Pathology, [3]Otolaryngology, Tulane University School of Medicine, USA; [4]Proteomics Research Program Unit, Basic Research Department, Children Cancer Hospital Cairo, Egypt; [5]Department of Physiology, Faculty of Veterinary Medicine, Suez Canal University, Ismailia 41522, Egypt; [6]Department of Pharmacology, Edward Via College of Osteopathic Medicine, University of Louisiana, Monroe, USA; [7]Department of Pharmacology, LSU Health Sciences Center, New Orleans, LA, USA. [*]Senior authors.

Received March 7, 2022; Accepted May 12, 2022; Epub July 15, 2022; Published July 30, 2022

Abstract: The presence of mutant BRAF^{V600E} correlates with the risk of recurrence in papillary thyroid cancer (PTC) patients. However, not all PTC patients with BRAF^{V600E} are associated with poor prognosis. Thus, understanding the mechanisms by which certain PTC patients with nuclear BRAF^{V600E} become aggressive and develop resistance to a selective BRAF inhibitor, PLX-4032, is urgently needed. The effect of nuclear localization of BRAF^{V600E} using *in vitro* studies, xenograft mouse-model and human tissues was evaluated. PTC cells harboring a nuclear localization signal (NLS) of BRAF^{V600E} were established and examined in nude mice implanted with TPC1-NLS-BRAF^{V600E} cells followed by PLX-4032 treatment. Immunohistochemical (IHC) analysis was performed on 100 PTC specimens previously confirmed that they have BRAF^{V600E} mutations. Our results demonstrate that 21 of 100 (21%) PTC tissues stained with specific BRAF^{V600E} antibody had nuclear staining with more aggressive features compared to their cytosolic counterparts. *In vitro* studies show that BRAF^{V600E} is transported between the nucleus and the cytosol through CRM1 and importin (α/β) system. Sequestration of BRAF^{V600E} in the cytosol sensitized resistant cells to PLX-4032, whereas nuclear BRAF^{V600E} was associated with aggressive phenotypes and developed drug resistance. Proteomic analysis revealed Arp2/3 complex members, actin-related protein 2 (ACTR2 aliases ARP2) and actin-related protein 3 (ACTR3 aliases ARP3), as the most enriched nuclear BRAF^{V600E} partners. ACTR3 was highly correlated to lymph node stage and extrathyroidal extension and was validated with different functional assays. Our findings provide new insights into the clinical utility of the nuclear BRAF^{V600E} as a prognostic marker for PTC aggressiveness and determine the efficacy of selective BRAF^{V600E} inhibitor treatment which opens new avenues for future treatment options.

Keywords: Thyroid cancer, BRAF^{V600E}, nuclear localization, Arp2/3 complex, ACTR2 (ARP2), ACTR3 (ARP3), vemurafenib resistance, poor prognosis

Introduction

Frequent mutations of the Ras-dependent RAF/MEK/ERK1/2 mitogen-activated protein kinase-signaling pathway lead to the development of malignancies, including melanoma and thyroid cancer (TC). Although its role in cancer progression is still controversial, *BRAF^{V600E}* has been associated with worse clinical outcomes in TC patients [1, 2]. The v-Raf murine sarcoma viral oncogene homolog B (BRAF) is activated in the cytoplasm when it binds to 14-3-3 protein dimers. Following the stimulation of cells by growth factors, BRAF binds to Ras protein, and then the translocates to the plasma membrane. Further activation of the kinase occurs by phosphorylation, which leads to activation of the MEK/ERK signaling pathway [3]. Growth factors constitutively activate BRAF but not the other kinase isoforms [4]. The *BRAF^{V600E}* mutation, a substitution of the amino acid valine by glutamic acid at position 600 in BRAF, accounts for 80-90% of all reported BRAF mutations [5].

Papillary TC (PTC) can progress to the more aggressive anaplastic variant (ATC), which is

associated with higher mortality rates [6]. ATCs that contain foci of PTC are generally positive for *BRAF^{V600E}*, implying that *BRAF^{V600E}* may play a role in the progression from PTC to ATC [7]. The incidence of *BRAF^{V600E}* mutation in PTC varies from 25% to 90%, and TC has a low mortality rate with up to a 98% overall five-year survival rate [8]. However, only 10-35% of undifferentiated ATCs harbor *BRAF^{V600E}* [1, 9-15]. Interestingly, not all TCs with *BRAF^{V600E}* are associated with poor prognosis [16-19]. We propose that this distinction may be related to BRAF^{V600E} cellular trafficking. This trafficking of the mutant kinase may prove to be a valuable prognostic marker of tumor progression and recurrence in PTC patients.

Vemurafenib (PLX-4032), a selective BRAF inhibitor, was FDA-approved for treatment of metastatic melanoma with *BRAF^{V600E}* [20-23] and was recently approved for aggressive PTCs and ATCs with *BRAF^{V600E}* [24]. Qualitative and quantitative data demonstrate the effectiveness and potency of some drugs to selectively inhibit TCs that harbor *BRAF^{V600E}* [25-29]. Although PLX-4032 has been shown to improve overall survival in patients with metastatic melanomas that harbor *BRAF^{V600E}*, the development of early resistance [30-36] is a major concern for patients with advanced TC. About 50% of patients developed an acquired resistance within seven months of treatment after initial response [37, 38].

TC patients at high risk for recurrence or development of resistance to selective BRAF inhibitors should receive an early and specific course of treatment; However, there are no reliable molecular markers to distinguish these patients. Thus, unraveling the underlying mechanisms by which TC cells with mutant *BRAF^{V600E}* become more aggressive, and identifying patients with *BRAF^{V600E}* at higher risk for recurrence, is critical and poorly studied. In this study, we aim to determine the biological significance of intranuclear BRAF^{V600E} in PTC cells, identify the molecular mechanisms by which TC cells with *BRAF^{V600E}* mutation become more aggressive and re-stratify TC patients with *BRAF^{V600E}* at higher risk of recurrence.

Materials and methods

Cell culture

Thyroid cancer SW1736 and KAT18 cells were obtained from Dr. N.E. Heldin (University of Uppsala, Sweden). NPA, melanoma cell line, was provided by Dr. G. Julliard (University California Los Angeles, CA). K1 cells were obtained from the Health Protection Agency Culture Collections (Salisbury, UK). TPC1 and MDA-T32 cells were kindly provided by Dr. Sato (Cancer Institute, Kanazawa University, Japan) and Dr. Clayman (MD Anderson Cancer Center, Houston, Texas), respectively. Nthy-ori 3-1 is a human immortalized follicular epithelial cell line derived from a normal thyroid (ECACC, Wiltshire, UK) [39]. BRAF$^{-/-}$ mouse embryonic fibroblast (MEF) cells were kindly provided by Dr. Baccarini (University Vienna, Austria) [40] and BCPAP (PTC cell line, PSMZ). Cells were cultured in DMEM medium (ThermoFisher Scientific, Waltham, MA) supplemented with 10% heat-inactivated fetal bovine serum (FBS), and 1% penicillin-streptomycin. Cells were maintained in a 37°C humidified incubator with 5% CO_2. The BRAF and NRAS mutation status for each cell line is summarized in Supplementary Table 1.

Cell proliferation and apoptotic assays

After reaching 70% confluence, cells were subcultured and seeded into 96-well plates (Corning Inc., NY). After overnight incubation, cells were treated with specific BRAF^{V600E} inhibitor PLX-4032 (Vemurafenib, SellekChem, Houston, TX) at concentrations ranging from 0 to 10 μM and at different time points. At the end of treatment, 10 μl of tetrazolium salt WST-8 (Cell Counting Kit-8, Dojindo Molecular Technologies Inc., MD) was added into the culture medium of cells [41]. The assay was executed in triplicate, and each experiment was independently repeated at least twice. For apoptotic assay, cells were treated with PLX-4032 (2 μM) for 48 h. Collected cells were washed and resuspended in PBS, and then annexin-V/propidium iodide (PI) was added (Annexin V-FITC Apoptosis Detection Kit, Sigma). Stained cells were analyzed by fluorescence-activated cell sorter (Flow Cytometry Core Facility, Tulane University School of Medicine, New Orleans, LA).

Clonogenic assay

Cells were plated at 100 cells per well in a 6-well plate in a complete DMEM medium. The following day, cells were treated with PLX-4032 (2 μM) or DMSO as a vehicle for 14 days. Cells were fixed and stained with a mixture of 50% methanol and 1% methylene blue.

Generation of nuclear localization signal (NLS)-BRAF^{V600E}-expressing clones

We established TC wild-type (WT)-BRAF cells expressing nuclear localization signal (NLS)-BRAF^{V600E} and BRAF^{V600E} as a control. Cells were infected with lentiviral particles expressing human BRAF^{V600E} with the following sequence: pLV[Exp]-Neo-CMV>DsRed_Express2: ORF_2373bp/Myc(hBRAF^{V600E}/3xNLS) or without NLS pLV[Exp]-Neo-CMV>DsRed_Express2: ORF_2301bp/Myc(hBRAF^{V600E}) tagged with DsRed fluorescent protein as per the manufacturer's instructions (Cyagen, Santa Clara, CA). Positive clones were selected under the pressure of antibiotic G418 (0.25 mg/ml). The expression of NLS-BRAF^{V600E} and BRAF^{V600E} in these clones was confirmed by immunofluorescence and Western blot analysis.

Immunoprecipitation, nuclear extraction, and Western blot analysis

Proteins from BCPAP, BCPAP-empty vector, BCPAP-BRAF^{V600E}, BCPAP-BRAF^{V600E}-3X NLS were lysed in Pierce IP lysis buffer mixed with protease inhibitors (ThermoFisher Scientific). The concentration of protein was estimated, and immunoprecipitation was performed using anti-DsRed2 Magnetic Beads following the standard protocol (Origene, TA183025). Eluted protein bands were subjected to long gradient LC-MS/MS analysis (Creative proteomics, NY, USA). Cell fractionations were isolated using the NE-PER kit from Pierce (Rockford, IL). For western blots, the following antibodies were used: Anti BRAF^{V600E} (Spring Bioscience), anti-GAPDH, anti-β-Actin, anti-Lamin B, anti-ACTR2, ACTR3 and F-actin (Santa Cruz Biotechnology, Dallas, TX, USA), anti-phospho-p44/42 ERK1/2, anti-ERK1/2, and anti-phospho-Akt (Cell Signaling, Beverly, MA).

In vivo studies

Inbred homozygous six-week-old athymic BALB/C nude female mice, provided by Charles River (Wilmington, MA, USA), were maintained in a pathogen-free barrier facility. Animal studies were performed in accordance with federal, local, and institutional guidelines and with approved IACUC protocol by Tulane University. Under a dissecting microscope, mice were orthotopically injected with 1.0×10^6 TPC-1 cells mixed with an equal amount of Matrigel™ (BD Bioscience, San Jose, CA) in thyroid gland as described [42]. Tumor growth was monitored every other day with measuring calipers. Tumor-bearing mice were randomly divided into two groups (five mice each): TPC-1 cells harboring NLS-BRAF^{V600E}, and TPC-1 cells harboring BRAF^{V600E}. About 50 mg/kg/day PLX-4032 (dissolved in 0.5% hydroxypropyl methylcellulose and 0.2% polysorbate 80) [43] in addition to 14 mg/kg/day G418 [44] dissolved in PBS were administered to each mouse by oral gavage every day for six weeks. Tumor volume was measured as previously described [45]. After six weeks, mice were sacrificed by euthanasia and tumor tissues were collected for further analyses.

Human TC tissue specimens

PTC tissue specimens were obtained from the Louisiana Cancer Research Center (LCRC) Biospecimen core following the approval of the Institutional Review Board (IRB) of Tulane University (Ref#2019-237). Clinicopathological data were retrospectively retrieved from patient records. Tissue microarray (TMA) slides for thyroid cancer (comprising 24 cases; Cat#Th721) were purchased from the US Biomax (US Biomax, Inc., Rockville, MD).

Immunohistochemical (IHC) analysis

FFPE PTC tissue blocks were cut into 4 μm thick slices, placed on glass slides, and stained with BRAF^{V600E} specific clone VE1 antibody as we previously described [46]. Briefly, tissue sections were deparaffinized, rehydrated and immunostained using Biocare reagents in a Biocare Nemesis 7200 automated system (Biocare Medical, Concord, CA). The endogenous biotin and hydrogen peroxide were quenched by sequential incubation in 3% H_2O_2 for 5 min and avidin-biotin blocking solution for 10 min. Antigen retrieval (Biocare BORG solution) was followed by the addition of VE1 (1:100 dilution) for 60 min. After incubation of tissues with secondary antibody, the developed signal was visualized by diaminobenzidine substrate (DAP)-chromogen solution. The slides were counterstained by hematoxylin and bluing solution. IHC scoring was performed and scored independently by two cytopathologists (ABS) and (KM) with perfect concordance (κ=1)

after double scope review of selected cases as previously described [47, 48].

Immunofluorescence analysis

Cells were cultured in chamber slides at regular and experimental conditions. At the end of each experiment, cells were fixed with 4% paraformaldehyde (Wako Laboratory Chemicals, Richmond, VA) for 10 min at room temperature. After washing with PBS, the cell membranes were permeabilized by treating the cells with Triton X-100 (0.1% wt/vol) in PBS for 15 min, and then cells were incubated with 5% BSA for 1 hour at room temperature. Cells were incubated overnight at 4°C with the specific primary antibody. Cells were rinsed thoroughly with PBS and incubated with Alexa Fluor® 594 or 488 secondary antibody. Cells were then stained with 4' 6'-diamindino-2-phenylindole (DAPI) and mounting medium (Vector Laboratories, Burlingame, CA). Images were recorded by an Olympus BX51 microscope equipped with epifluorescence optics and an Olympus camera (Olympus America Inc., Center Valley, PA).

Nano LC-MS/MS analysis

In this experiment, four samples (BCPAP, BCPAP-empty vector, BCPAP-BRAF^{V600E}, BCPAP-BRAF^{V600E}-3X NLS) were subjected to digestion with trypsin, and were analyzed on a high-resolution mass spectrometry analysis coupled with nanoflow UPLC. An Ultimate 3000 nano UHPLC system coupled with a Q Exactive HF mass spectrometer (Thermo Fisher Scientific, USA) with an ESI nanospray source was used to analyze the samples.

Bioinformatics analysis

Protein outputs retrieved from MaxQuant for all experimental groups (BCPAP, BCPAP-empty vector, BCPAP-BRAF^{V600E}, BCPAP-BRAF^{V600E}-3X NLS) were analyzed using ProteoCompanion, an in-house R-based software to analyze protein differential expressions among groups [49]. A total of 142 unique proteins in the NLS group were further tested for gene ontology and pathway analysis (Reactome, KEGG) using uniprotR package [50]. For significant pathways, an adjusted *p*-value was considered significant at P<0.05 as shown in **Figure 7**.

Statistical analysis

Data are presented as mean ± SEM. Comparisons between different groups were performed using Student's *t*-test or ANOVA with a Bonferroni test. Data were considered significant at *p*-value <0.05. We utilized SAS 9.3 software to perform the statistical analyses related to this study.

Results

Detection of BRAF^{V600E} nuclear staining in PTC patient tissues

We identified nuclear versus cytoplasmic staining of BRAF^{V600E} by IHC using VE1 antibody (**Figure 1A1**, **1A2**). Non-counterstained PTC tissue sections were used to confirm the nuclear staining (**Figure 1A3**: solid arrow) versus cytosolic (**Figure 1A4**: arrowhead). Out of 100 BRAF^{V600E}-postive human PTC tissue specimens confirmed by PCR as we described [46], 21 (21%) displayed positive nuclear BRAF^{V600E} (**Figure 1B**). Interestingly, overall BRAF^{V600E} nuclear staining was mostly detected in FVPTC (42.9%) and TCVPTC (41.7%), in comparison to CVPTC (18.5%) tissue sections as shown in **Figure 1B**. Importantly, nuclear BRAF^{V600E} in our cohort was correlated with the presence of high-risk prognostic features. Patients with nuclear BRAF^{V600E} had aggressive variants such as tall-cell variant, lateral lymph node metastasis (N1b), recurrence, and higher ATA risk stratification criteria.

Identification of nuclear localization of BRAF^{V600E} in thyroid cancer cells

We and others recently used a specific BRAF^{V600E} antibody in human PTC tissues and reported that BRAF^{V600E} is localized in the nucleus of some PTC cells [46, 51]. The persistence of such BRAF^{V600E} nuclear localization prompted us to examine whether nuclear BRAF^{V600E} has any biological or clinical significance in PTC cells. We initiated our study by staining a large panel of TC cells that harbor either WT BRAF or BRAF^{V600E}. Under normal conditions, BRAF^{V600E} was detected in the nuclei of BRAF^{V600E}-positive PTC K1 but not in normal thyroid Nthy-ori-3-1 cells (WT-BRAF) as shown in **Figure 2A**. The ATC cell line SW1736 displayed an exclusively cytosolic BRAF^{V600E}. The difference of BRAF^{V600E} localization in K1

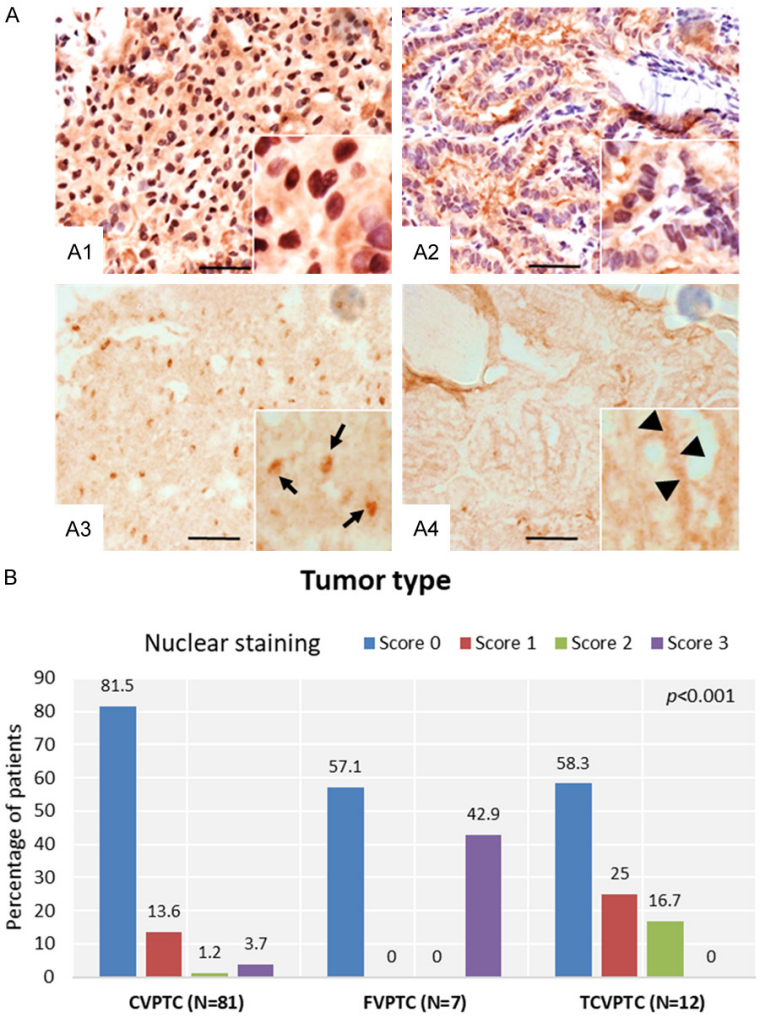

Figure 1. Representative photomicrographs of human PTC tissue sections showing nuclear staining of BRAF^{V600E}. A: After validating the PTC tissue by H&E staining, nuclear and cytoplasmic localization of BRAF^{V600E} was detected by immunostaining using anti-VE1 antibody (A1, A2). Non-counterstained PTC tissues sections were used to confirm the nuclear staining (A3: solid arrows) versus cytosolic (A4: arrowheads). Scale bar is 50 µm. B: Relationship between thyroid tumor type and BRAF^{V600E} nuclear staining.

and SW1736 cells could be related to mutations and response to Vemurafenib. Though K1 has BRAF, TERT, PIK3CA mutations and IC_{50} of 0.827 µM to vemurafenib, SW1736 has BRAF, TERT, p53, TSHR mutations and IC_{50} of 0.115 µM [27]. The specificity of BRAF^{V600E} antibody (VE1 clone) was examined by western blot analysis in different TC cells (**Figure 2B**) including one melanoma cell line, NPA [27, 52]. The nuclear localization of BRAF^{V600E} in PTC K1 cells growing in regular culture medium (presence of FBS) was confirmed by cell fractionation followed by immunoblot analysis (**Figure 2C**). A list of TC cells and mouse embryonic fibroblasts (MEF) used in the current study indicating BRAF and NRAS mutation status is presented in Supplementary Table 1.

BRAF^{V600E} translocates to the nucleus upon growth factor stimulation in BRAF^{V600E}-positive PTC cells

Although we were able to show that BRAF^{V600E} is localized in the nucleus of PTC cells, we still lacked information on the mechanism of translocation from the cytosol to the nucleus and its biological significance in cancer cells. Since BRAF is a growth factor-stimulated kinase, we set out to examine whether removal or addition of growth factors would translocate BRAF^{V600E} from the nucleus to the cytosol. Interestingly, removal of growth factors upon serum (FBS) starvation for 48 hours promoted an exclusively cytoplasmic BRAF^{V600E} in K1 cells (**Figure 3A**), and subsequent stimulation of these cells with serum (10% FBS) for 24 hours induced nuclear translocation of BRAF^{V600E}. This finding was confirmed by cell fractionation followed by immunoblot analysis (**Figure 2C**). To examine whether a specific growth factor controls the translocation of BRAF^{V600E} from cytosol to the nucleus, cells were first starved for 36 h then treated with 10 ng/ml of insulin-like growth factor-1 (IGF-1) at different time intervals. The selection of IGF-1 is based on a recent publication revealing that the activation of IGF-1 receptor (IGF1R) in melanoma BRAF-mutant cell lines mediates resistance to dabrafenib and trametinib and patients with high levels of IGF1R have worst survival outcomes [53]. Moreover, p300-mediated acetylation occurs on both wild type (WT)- and V600E-BRAF and could be induced by insulin, which activates p300 through the phosphatidylinositol 3-kinase (PI3K)/AKT signaling path-

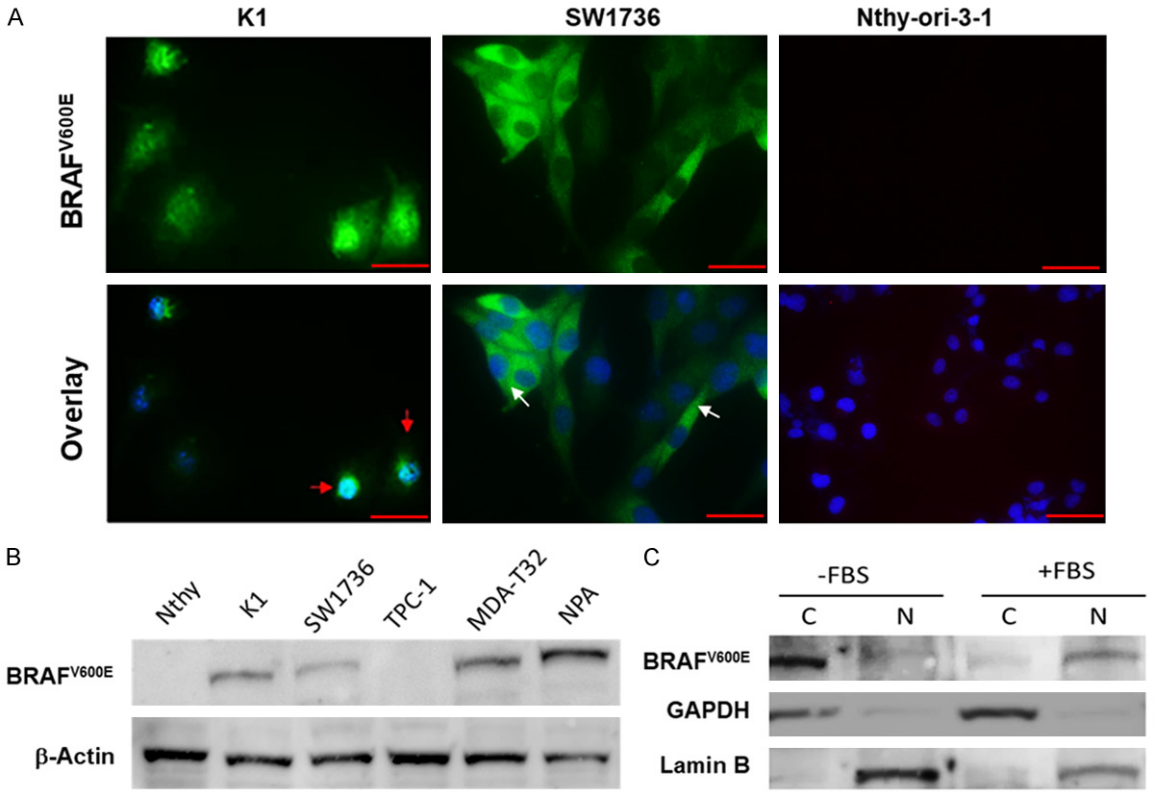

Figure 2. Nuclear localization of BRAF^{V600E} in thyroid cancer cells. A: K1 (PTC) and SW1736 (ATC) and Nthy-ori-3-1 (normal) cells were grown in a complete RPMI-1640 medium. Cells were fixed with 4% paraformaldehyde, blocked with 1% BSA followed by staining with anti-BRAF^{V600E} (VE1 antibody; Spring Bioscience) specific antibody and then visualized by fluorescence microscopy. Red and white arrows indicate nuclear and cytosolic localization of BRAF^{V600E}, respectively. Nthy-ori-3-1 (WT-BRAF) did not show any staining. Magnification is 400X. Scale bar =20 μm. B: Expression of BRAF^{V600E} in a panel of thyroid cancer cell lines using Western blot analysis. C: Nuclear and cytosolic fractions were collected from K1 cells after serum starvation for 24 h followed by adding 10% FBS into the medium for another 24 h. Western blot was performed as indicated using VE1, anti-lamin B and anti-GAPDH antibodies. C: Cytosolic, N: Nuclear fractions.

way [54]. **Figure 3B** shows that IGF-1 exposure was more efficient than FBS for inducing nuclear translocation of BRAF^{V600E}. Nuclear translocation of BRAF^{V600E} was observed as early as one hour after stimulation. These findings suggest that the nuclear translocation of BRAF^{V600E} is a dynamic biological process.

Subcellular trafficking of BRAF^{V600E} is mediated by CRM-1 and importin-α/β

The mechanism of nuclear import and export is a key factor in cell homeostasis and often an important player in cancer when the transport machinery is dysregulated [55, 56]. Taking this into consideration, it is necessary to determine whether such machinery is critical for BRAF^{V600E} subcellular trafficking in PTC cells. Initially, K1 cells were serum-starved for 48 h followed by the addition of serum for 24 h to promote nuclear translocation of BRAF^{V600E} as shown in **Figure 3A**. Next, cells were starved for another 4 h in the absence or presence of 5 ng/ml of the specific CRM1 inhibitor leptomycin B (LMB). Interestingly, BRAF^{V600E} remained in the nucleus upon CRM1 inhibition compared to its cytosolic localization in the absence of LMB (**Figure 4A**). This is the first evidence to show that translocation of BRAF^{V600E} from the nucleus to the cytosol is CRM1-dependent. We then investigated whether nuclear importing of BRAF^{V600E} is dependent on importins. We examined the effect of inhibiting the nuclear import system on BRAF^{V600E} subcellular localization. This was achieved by cell starvation for 24 h followed by adding 10 ng/ml IGF-1 into the medium for 6 h in the presence or absence of 10 μM ivermectin, a specific inhibitor of

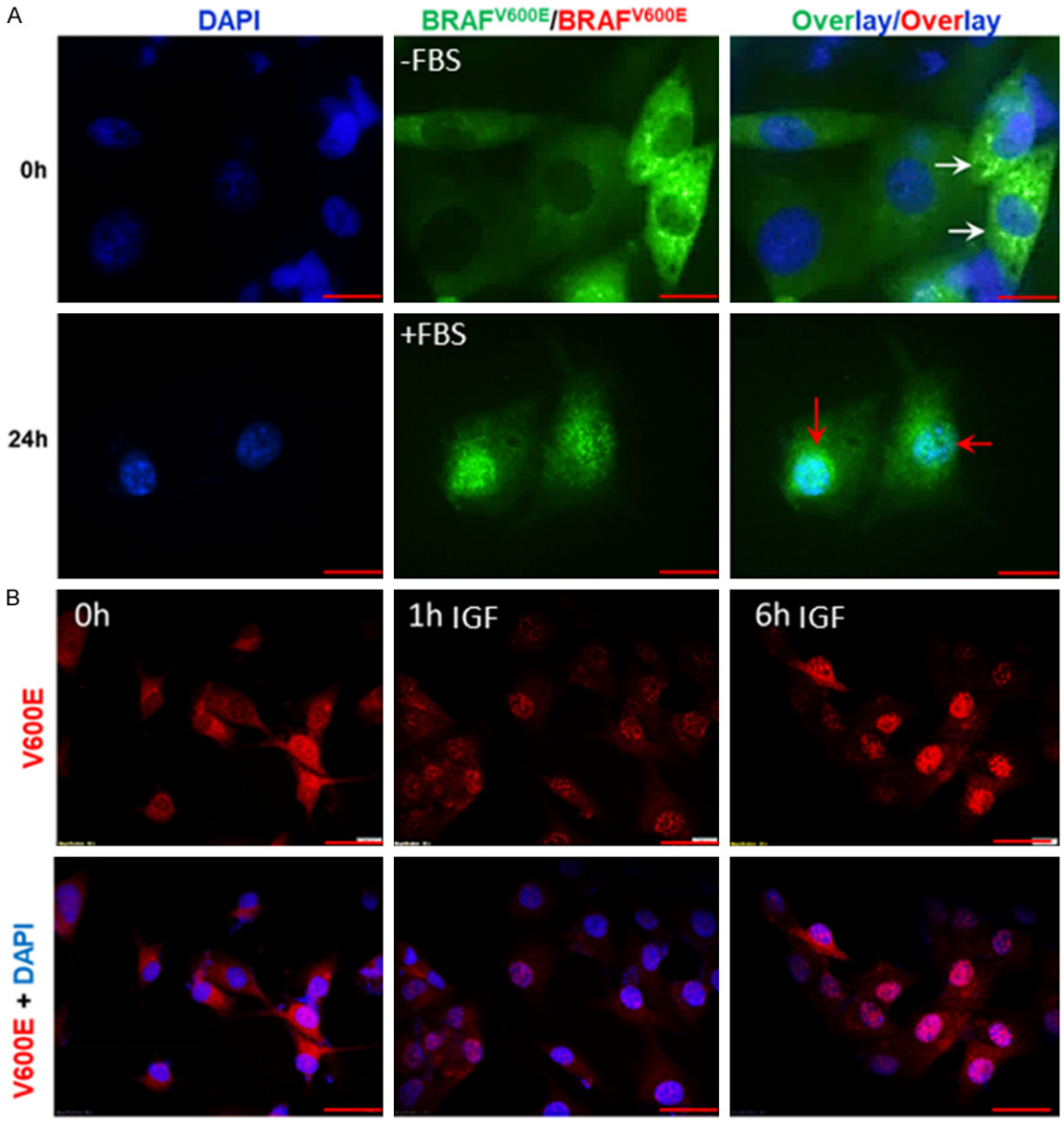

Figure 3. Dynamic translocation of BRAF^{V600E} in K1 cells is a growth factor-dependent process. A: Cellular localization was monitored after serum depletion for 48 h followed by serum stimulation for another 24 h. BRAF^{V600E} was enforced to translocate to cytosol (white arrows) after serum depletion for 48 h (upper panel) and then moved back to the nucleus (red arrows) after serum stimulation for 24 h (lower panel). Magnification was 400X. Scale bar is 10 μm. B: Cells (harboring BRAF^{V600E}) were serum-starved for 36 h followed by the addition of 10 ng/ml IGF-1 in culture medium for 1 and 6 h. Cells were fixed and stained as indicated. Scale bar is 20 μm.

importin α/β [57]. In fact, translocation of BRAF^{V600E} into the nucleus upon IGF-1 stimulation was completely blocked by treating cells with an importin inhibitor (**Figure 4B**). These findings suggest that subcellular localization of BRAF^{V600E} is dynamic and controlled by the export/import machinery in BRAF^{V600E}-positive cancer cells.

Sequestration of BRAF^{V600E} in the nucleus increases aggressive cell behavior and develops resistance to vemurafenib in thyroid cancer cells

In prior experiments, we were able to demonstrate that BRAF^{V600E} is dynamic and controllable. However, serum starvation may affect cel-

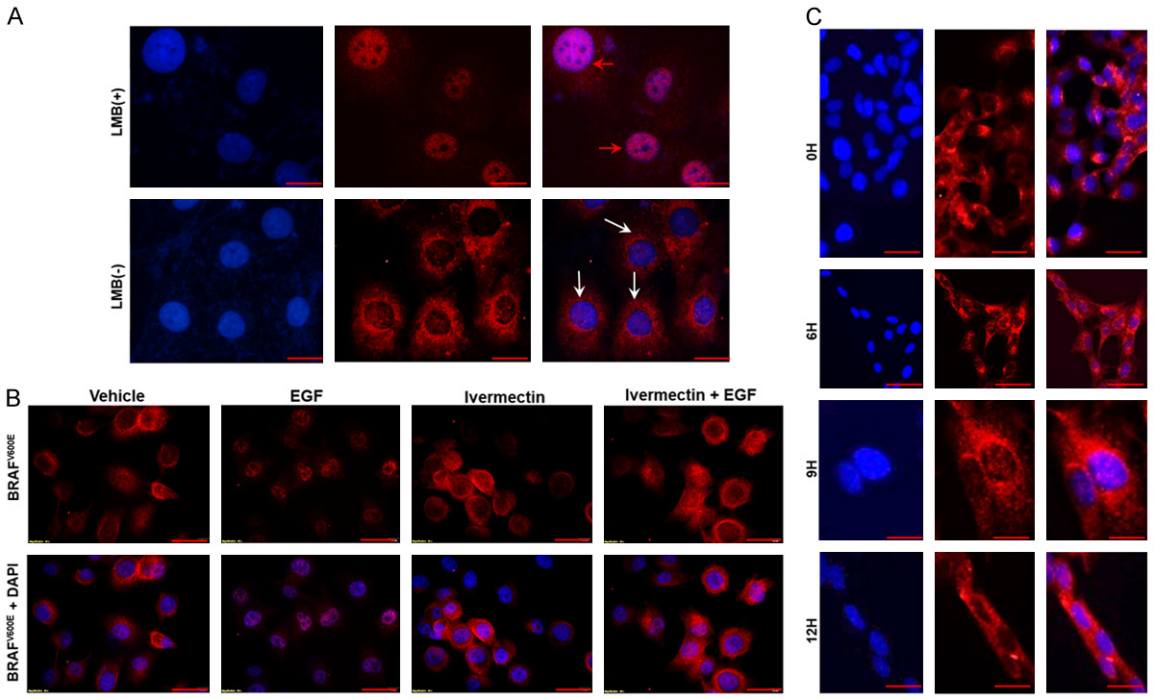

Figure 4. Cytosolic localization of BRAF^{V600E} is CRM-1 dependent while nuclear translocation is importin α/β dependent. A: CRM-1 inhibitor (Leptomycin B; LMB; 5 ng/ml) was applied as indicated. K1 cells were starved for 48 h, serum stimulated for 24 h and then depleted for 48 h with and without applying LMB. Scale bar is 10 μm. B: In another experiment, cells were deprived of serum for 36 h, followed by 10 μM ivermectin (importin selective inhibitor) treatment in serum-free medium for 4 h and then 10 ng/mL IGF-1 alone and in combination with ivermectin were added to the culture medium for another 6 h. Cells were fixed and stained with VE1 antibody, and nuclei were stained with DAPI. Magnification is 400X. C: In TPC1 cells, WT BRAF cellular localization was monitored after serum depletion for 48 h followed by serum stimulation for another 12 h. No WT BRAF nuclear translocation was observed up to 12 h. Magnification was 400X. Scale bar is 20 μm.

lular activities, which could complicate our plan to examine the effect of BRAF^{V600E}-specific inhibitor on nuclear localization of BRAF^{V600E}. To prevaricate this confounding condition, we generated a lentiviral vector in which *BRAF^{V600E}* was inserted in-frame with a sequence encoding DsRed2, which encodes a red fluorescent protein followed by BRAF^{V600E} and three nuclear localization signal (3X NLS) domains. KAT18 and TPC1 cells were infected by vectors carrying NLS-BRAF^{V600E}, BRAF^{V600E}, or NLS alone as a negative control. WT BRAF (KAT18 and TPC1) and not mutant BRAF cell lines were chosen to evade having endogenous and exogenous BRAF^{V600E} expression in the same cells after BRAF^{V600E} or NLS-BRAF^{V600E} transduction. The efficiency of infection was shown by western blot analysis (**Figure 5A**) and immunofluorescence staining (**Figure 5B**). Applying the same approach, we also infected mouse embryonic fibroblast (MEF$^{BRAF-/-}$) cells that lack BRAF as described [58]. The sensitivity of these stably transduced cells towards the BRAF^{V600E}-specific inhibitor vemurafenib (PLX-4032) was examined. Cells were incubated with different concentrations of PLX-4032 for five days (1-10 μM), and cell viability was assessed by the WST-8 assay. As expected, stably BRAF^{V600E}-expressing KAT18 (ATC) and MEF^{BRAF} cells (BRAF^{V600E} localized in the cytosol) showed a remarkable sensitivity to PLX-4032 compared to their parental cells, which have a WT-BRAF. Strikingly, NLS-BRAF^{V600E}-expressing cells (BRAF^{V600E} localized in the nucleus) provided substantial resistance to PLX-4032 treatment. These results were also validated using colonogenic assay with KAT18 and MEF^{BRAF} (**Figure 5C** and **5D**). Inhibition of ERK phosphorylation is a major mechanism by which vemurafenib exerts its effect on BRAF^{V600E}-positive cells [59]. Thus, the activity of ERK1/2 was examined in KAT18 and another WT BRAF cell line (PTC-1) where BRAF^{V600E} is localized in the nucleus. Cells harboring NLS-BRAF^{V600E} (nuclear) exhibited an

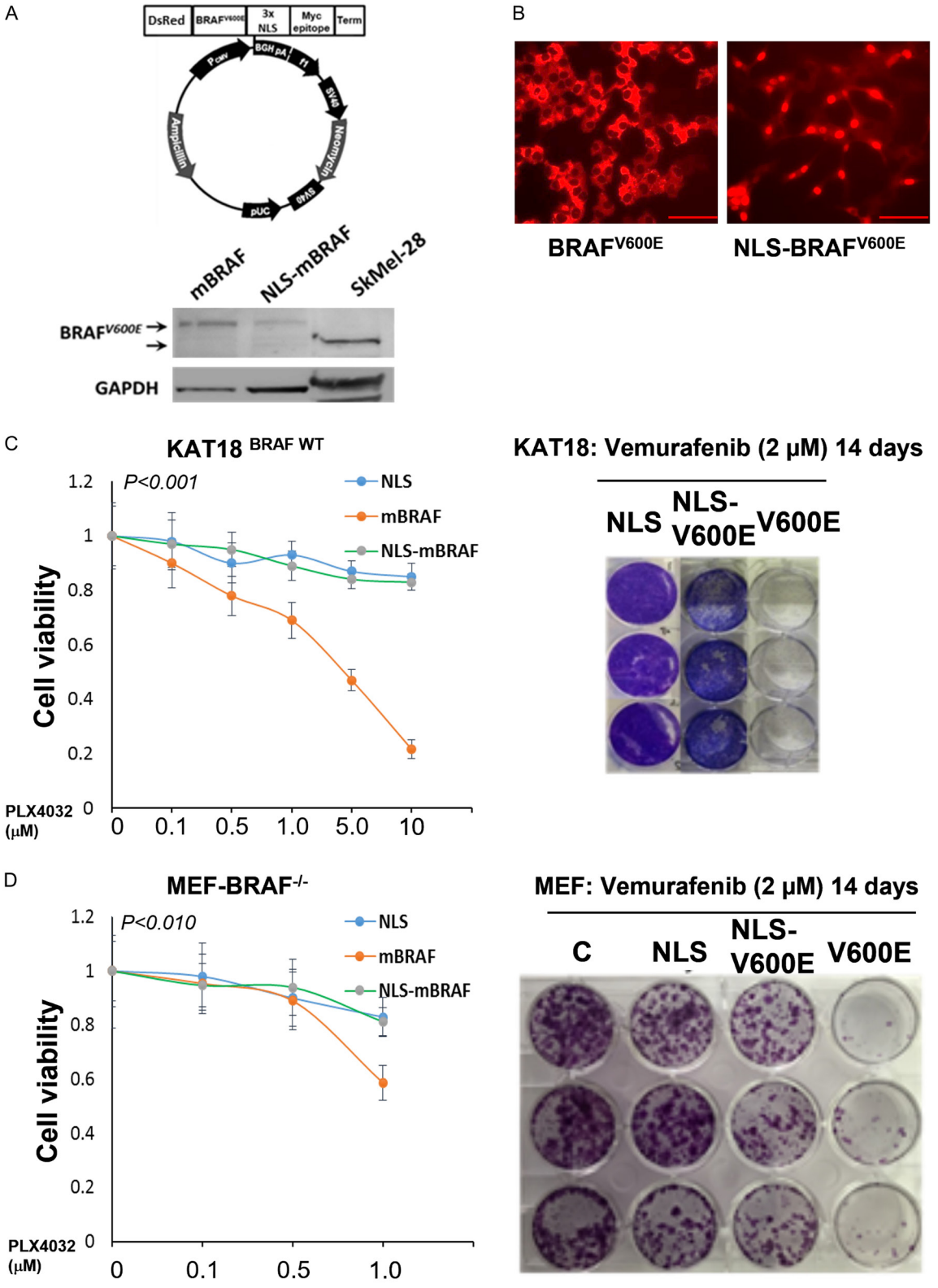

Figure 5. Nuclear localization of BRAF^{V600E} induces vemurafenib resistance in thyroid cancer KAT-18 cells and MEF-BRAF$^{-/-}$. A: Cells were transfected with NLS-BRAF^{V600E}, BRAF^{V600E} or NLS (as a control vehicle) plasmid under G418 selection. Clones were examined by Western blot analysis using anti-VE1 antibody and loading control anti-GAPDH. B: NLS-BRAF^{V600E}- and BRAF^{V600E}-positive cells were stained with VE-1 antibody and examined under a fluorescence

microscope. Scale bar is 20 μm. C and D: Equal numbers of NLS-BRAF^{V600E}, BRAF^{V600E} and NLS-harbored MEF$^{BRAF-/-}$ and KAT18 cells were cultured and treated at different concentrations of PLX-4032 for 5 days. Cell viability was assessed by WST-8 assay and the developed color was measured at 450 nm. In another experiment, 100 cells were cultured in 6-well plates and treated with 2 μM of PLX-4032 for 14 days, fixed and stained with crystal violet. * indicates significance at P<0.010. Experiments were repeated at least twice.

early ERK1/2 phosphorylation, and treatment with PLX-4032 did not reduce ERK1/2 activity but was persistent up to 48 h after treatment. In fact, PLX-4032 did not inhibit the activity of ERK1/2 at early time points (2 h, 6 h) in NLS-BRAF^{V600E}-harboring cells (**Figure 6A**). TPC1-NLS-BRAF^{V600E}-expressing cells exerted a similar phosphor ERK1/2 pattern after PLX4032 treatment (**Figure 6B**). KAT18 cell cycle analysis demonstrated that PLX-4032 suppressed S-phase by 50% in BRAF^{V600E}-harboring cells, whereas NLS-BRAF^{V600E}-carrying cells had a 22% reduction in S-phase compared to control cells (**Figure 6C**).

Nuclear BRAF^{V600E} develops PLX-4032 resistance in a TC preclinical model

To confirm the *in vitro* results, we used a xenograft mouse model to examine the effect of PLX-4032 on nuclear BRAF^{V600E}. TPC-1 cells expressing BRAF^{V600E} or NLS-BRAF^{V600E}, validated from *in vitro* studies, were orthotopically inoculated into thyroid glands of female nude mice. After tumors became palpable, animal groups were treated with PLX-4032 as indicated in the methods, and tumor growth was monitored for six weeks. Surprisingly, NLS-BRAF^{V600E}-harboring TPC-1 thyroid injected cells produced a substantial increase in tumor size compared to mice injected with BRAF^{V600E}-expressing cells (**Figure 6D**).

Nano LC-MS/MS and bioinformatics analysis: detection of ACTR2 and ACTR3 as exclusive partners of nuclear BRAF^{V600E}

By employing nano-liquid chromatography-tandem mass spectrometry deep proteomics technology and advanced bioinformatics algorithms, we comparatively examined the respective proteomic contents of BCPAP, BCPAP-empty vector, BCPAP-BRAF^{V600E}, and BCPAP-NLS-BRAF^{V600E}. BCPAP cell line was carefully chosen for gender and age reasons. It originated from a 76-year-old female and these two factors are crucial in TC. Protein profiles retrieved from MaxQuant for all experimental groups were analyzed using ProteoCompanion, an in-house R-based software to analyze differential protein expressions among groups (**Figure 7A**) [49]. Unique proteins in the NLS group (142 accession) were further tested for gene ontology and pathway analysis (Reactome, KEGG) using uniprotR package (**Figure 7B**), and for the cellular component, molecular function and biological processes (**Figure 7C**) [50]. For significant pathways, an adjusted *p*-value was considered significant at P<0.05.

Knockdown of ACTR3 has a tumor suppressor effect in TC cells

The top 10 protein partners of nuclear BRAF are presented in the **Figure 8A** and a validation of ACTR3 protein expression by western blot in total proteins is shown in **Figure 8B**. We next validated, by immunofluorescence, the nuclear colocalization of ACTR2 and ACTR3 with nuclear BRAF^{V600E} in BCPAP cells. **Figure 8C** shows a clear colocalization in a particular region of the nucleus that could be the nuclei. Our bioinformatic analysis showed that only ACTR3 is related to thyroid metastasis. Upregulation of ACTR3 has the highest *p*-values (P=1.01E-05 for lymph node stage (N1 vs N0) and P=0.013 for extrathyroidal extension (ETE)) compared to ACTR2 (P=0.002 and P=0.084). We then established a stable BCPAP cell line with ACTR3 knockdown by using ACTR3 shRNA lentiviral particles as recommended by Santa Cruz's protocol. Next, we selected stable clones that express shRNA via puromycin dihydrochloride. To confirm ACTR3 knockdown, we performed western blot analyses and were surprised to observe that ACTR2 protein expression was reduced after ACTR3 knockdown (**Figure 8D**). No effect was observed on BRAF protein expression in the BCAPAP/ACTR3 knockdown. Interestingly, in MEF cells, BRAF knockout slightly reduced ACTR3 protein expression and to a greater extent ACTR2 protein expression (**Figure 8E**). In an invasion assay, we found that silencing of ACTR3 (and consequently ACTR2) decreased cell invasion by about 35% (**Figure 8F**). Moreover, the colony formation assay with BCPAP showed a reduced ability of a single cell to grow

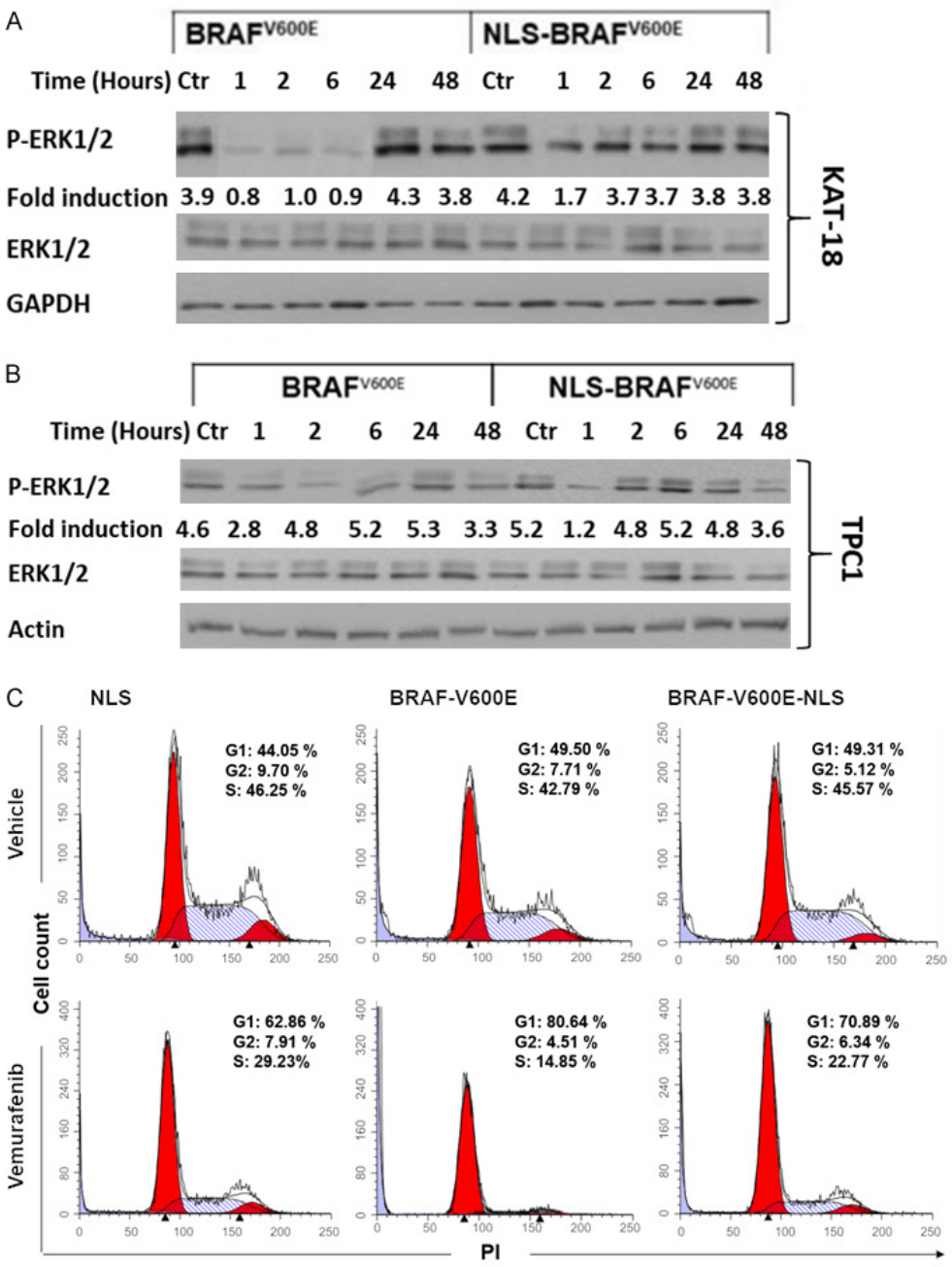
A
BRAFV600E
NLS-BRAFV600E
Time (Hours) Ctr 1 2 6 24 48 Ctr 1 2 6 24 48
P-ERK1/2
Fold induction 3.9 0.8 1.0 0.9 4.3 3.8 4.2 1.7 3.7 3.7 3.8 3.8
ERK1/2
GAPDH
KAT-18
B
BRAFV600E
NLS-BRAFV600E
Time (Hours) Ctr 1 2 6 24 48 Ctr 1 2 6 24 48
P-ERK1/2
Fold induction 4.6 2.8 4.8 5.2 5.3 3.3 5.2 1.2 4.8 5.2 4.8 3.6
ERK1/2
Actin
TPC1
C
NLS
BRAF-V600E
BRAF-V600E-NLS
Vehicle
Vemurafenib
Cell count
G1: 44.05 %
G2: 9.70 %
S: 46.25 %
G1: 49.50 %
G2: 7.71 %
S: 42.79 %
G1: 49.31 %
G2: 5.12 %
S: 45.57 %
G1: 62.86 %
G2: 7.91 %
S: 29.23%
G1: 80.64 %
G2: 4.51 %
S: 14.85 %
G1: 70.89 %
G2: 6.34 %
S: 22.77 %
PI

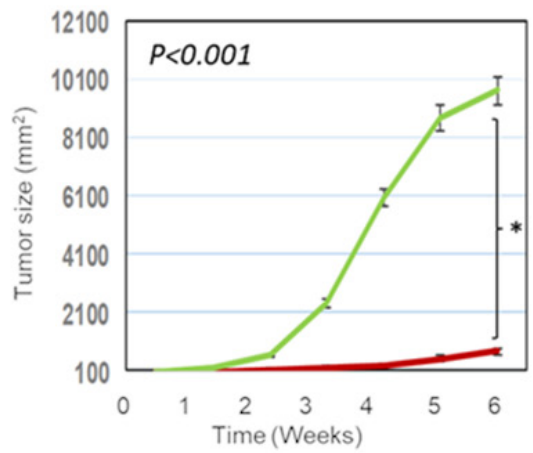
D
P<0.001
Tumor size (mm2)
Time (Weeks)
12100
10100
8100
6100
4100
2100
100
0 1 2 3 4 5 6
*


mBRAF
NLS-mBRAF

Figure 6. Nuclear localization of BRAF^{V600E} promotes vemurafenib resistance and tumor growth in thyroid cancer mouse model. (A, B) ERK1/2 activity was assessed by its phosphorylation in stably transfected BRAF^{V600E} or NLS-BRAF^{V600E} cells after treating KAT18 (A) and TPC-1 (B) cells with 5 μM PLX-4032 or DMSO at different time points. (C) KAT18 cells transduced with lentiviral vectors carrying NLS-BRAF^{V600E}, BRAF^{V600E} or NLS followed by vemurafenib treatment for 24 h and then fixed and stained with PI to evaluate the effect of nuclear BRAF^{V600E} on cell cycle using flowcytometric analysis. (D) Female nude mice (five mice per group) were orthotopically injected in thyroid gland with TPC-1 cells transduced with either NLS-BRAF^{V600E} or BRAF^{V600E} (1×10^6 cells/mouse). Tumor size was monitored twice a week for 6 weeks during vemurafenib treatment (50 mg/kg/day). * indicates significance at P<0.010.

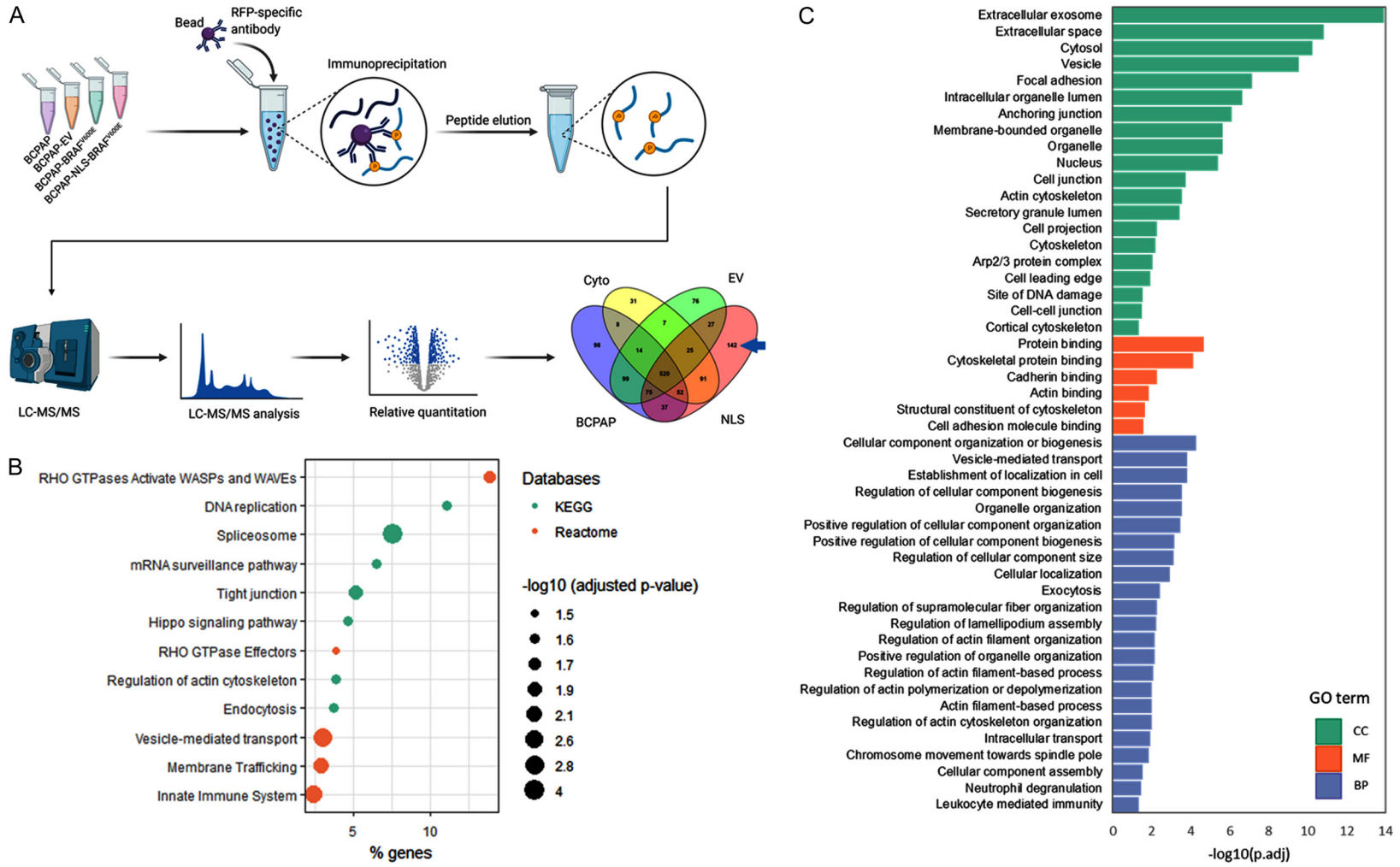

Figure 7. Mass spectrometry analysis: detection of ACTR2 (ARP2) and ACTR3 (ARP2) as an exclusive partner of nuclear BRAF^{V600E}. A: BCPAP, BCPAP-empty vector, BCPAP-BRAF^{V600E}, and BCPAP-BRAF^{V600E}-3X NLS were subjected to mass spectrometry analysis, and the 142 unique partners of nuclear BRAF were selected. B: 142 unique proteins were subjected to KEGG and reactome analysis. C: 142 proteins were segregated b/ased on their gen ontology (GO); cellular component (CC), molecular function (MF), and biological process (BP) analyses.

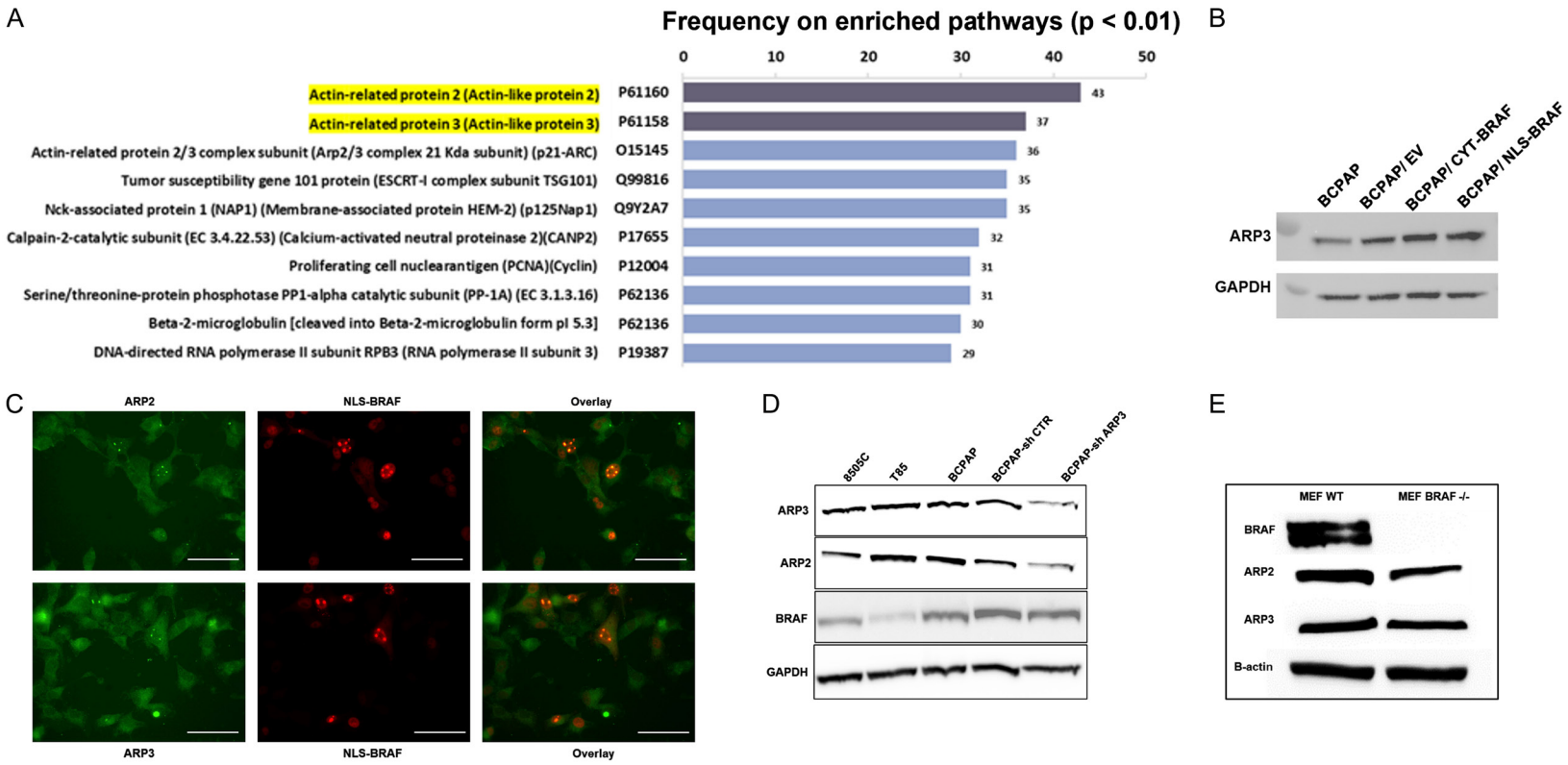

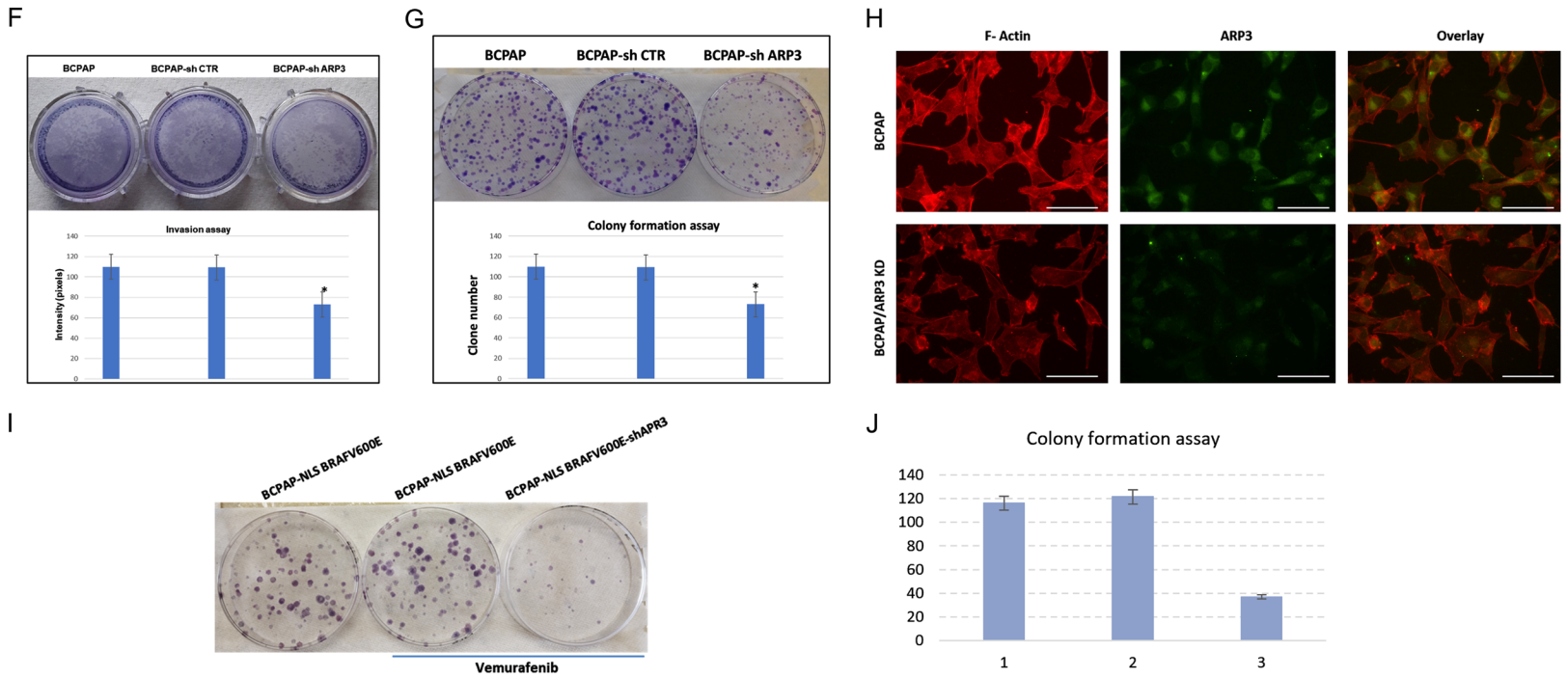

Figure 8. Knockdown of ACTR3 (ARP3) has a tumor suppressor effect in resistant TC cells. A: The top 10 protein partners of nuclear BRAF. B: Validation of ACTR3 protein expression by western blot in total proteins. C: Validation of ACTR2 and ACTR3 colocalization with nuclear BRAF in BCPAP cells by immunofluorescence. D: The protein levels of BRAF, ACTR2, and ACTR3 were assessed in BCPAP cells with knockdown of ACTR3. Parental BCPAP, 8505C and T85 cell lines were used as controls. E: The protein levels of BRAF, ACTR2, and ACTR3 were assessed in MEF WT and MEF BRAF$^{-/-}$. F: Cell migration was evaluated by using invasion assay in BCPAP cells with ACTR3 knockdown. All assays were performed in triplicate. *P<0.002. G: Representative colony formation of BCPAP cells with ACTR3 knockdown. The assay was done in triplicate. **P<0.002. H: Immunofluorescence after F-Actin staining of BCPAP and BCPAP/ACTR3 knockdown cells. Scale bar is 20 μm. I: Representative colony formation of BCPAP-NLS BRAF cells with ACTR3 knockdown and treated with vemurafenib. The assay was performed in triplicate and ** denotes P<0.001. J: Quantification of the colony formation assay.

into a colony when ACTR3 was knocked down (**Figure 8G**). No significant deregulation in the F-actin was observed after ACTR3 knockdown (**Figure 8H**). The resistant form of BCPAP to vemurafenib treatment (BCPAP-NLS-BRAF) was treated with 1 M of vemurafenib for 14 days before and after knocking down ACTR3. **Figure 8I** and **8J**, show a significant reduction of the clone formation when ACTR3 expression is reduced by specific shRNA against ACTR3 gene.

Discussion

In addition to our previous study [46], BRAF^{V600E} immunostaining has been also identified in the nucleus of different tumor tissues, but its clinical significance has never been investigated in TC [51, 60, 61]. During the course of IHC study [46], we stained FFPE tissue sections with BRAF^{V600E}-specific antibody and identified nuclear staining of BRAF^{V600E} in PTC tissues. Similar findings in melanoma tissue sections were recently published by our group [62]. This recognition promoted us to closely examine whether this phenomenon is actually dynamic, which may present us with an opportunity to not only understand the pathophysiological consequences of such unusual subcellular localization but also to determine the underlying mechanisms through which PTC cells harboring BRAF^{V600E} develop resistance to the selective BRAF inhibitor vemurafenib. A growing body of evidence suggests that several tumor suppressor proteins exhibit a change in their subcellular localization, a condition in which the tumor suppressor activity may be compromised. The transport of these proteins from the nucleus to the cytosol is mediated by CRM-1 [63] while other proteins are transported from the cytoplasm to the nucleus by importins [64]. Under certain pathological conditions, these factors promote cellular abnormalities by changing protein expression, incidence of mutations in importin-α/-β, or disruption of the RanGTP/GDP [65]. Some cancer cells take advantage of the normal cellular processes of nuclear-cytoplasmic transport to effectively develop resistance to established therapies [56, 60, 63, 66].

Our *in vitro* results demonstrate that nuclear localization of the kinase was identified only in BRAF^{V600E} but not in wild-type BRAF-bearing PTC cells, which implies that such a transport mechanism is selective to the mutant kinase. The utility of the BRAF^{V600E}-specific antibody VE1 was validated in a wide variety of tumors in several studies including ours [46, 61, 67-70]. In support of the immunofluorescence results, BRAF^{V600E} was also recognized in the nuclear fraction of TC cells under normal conditions. Upon growth IGF-1 stimulation, BRAF^{V600E} is dynamically regulated by the removal or addition of this factor to culture medium, and such translocation takes place within hours. By inhibiting proteins involved in the cell transport system, BRAF^{V600E} was found to be transported from the nucleus to the cytosol through CRM-1, and from the cytosol to the nucleus via the importin-α/β system. One increasingly common strategy for deterring cancer growth and progression is to target the nuclear transport system. Targeting CRM-1 revealed a reduction in tumor growth regardless of BRAF or NRAS status and resulted in a significant regression of tumor mass when combined with vemurafenib [63]. However, therapeutic targeting of nucleo-cytoplasmic transport is limited, because both normal and cancer cells have common mechanisms associated with cell transport machinery.

Remarkably, the sequestration of BRAF^{V600E} in the cytosol sensitizes TC cells to vemurafenib, and nuclear localization of the kinase increased drug therapy resistance of KAT18 and MEF-BRAF$^{-/-}$ cells. This was also evidenced by extending ERK1/2 activation in the presence of vemurafenib. A continuous but not transient ERK activation is connected to its nuclear localization, suggesting that the differential activation of ERK may be a determinant factor for eliciting a specific biological effect [4]. Thus, the cellular compartments of RAS/RAF/MEK/ERK are very important for exerting a certain biological role during normal and pathological conditions. Extended ERK activation in cells took place in the absence of the cytoplasmic RAS-MEK, suggesting a novel mechanism for resistance: Most likely, nuclear BRAF^{V600E} adapts cellular mechanisms to escape ve murafenib and gain resistance even after combination therapy is applied [71]. Targeting BRAF^{V600E} and cyclin-dependent kinases CDK4/6 in aggressive PTC cells is a new approach to reduce intrinsic or acquired resistance to vemurafenib [72]. Orthotopic injection of mice with nuclear BRAF^{V600E}-harboring cells produced larger tumor size than cells harboring cytosolic BRAF^{V600E}. In PTC tissue specimens, we were able to recognize BRAF^{V600E} in

the nucleus of tumor cells. We also showed that the incidence of nuclear BRAF^{V600E} in PTC subtypes is varied. Nuclear BRAF^{V600E} was detected in about 40% of tall cell variant (TCV) PTCs, which implies a contribution of nuclear BRAF^{V600E} to advanced tumors. It is known that PTC patients with tall-cell variants have poor prognosis compared to conventional variant and follicular variant subtypes [73]. In a recent study conducted on a large number of TC tissue specimens collected from 11 medical centers, BRAF^{V600E} was able to segregate solitary intrathyroidal PTC patients with higher risk of recurrence [74]. This study highlights the anticipated role of BRAF^{V600E} in TC aggressiveness. As expected, the relative lower incidence of nuclear BRAF^{V600E} in PTC tissues, if the low staining intensity of BRAF^{V600E} (intensity 1) was excluded, is suggested to be linked with low mortality rate in PTC patients [8]. By using mass spectrometry, we discovered proteins interacting exclusively with nuclear but not cytosolic BRAF^{V600E}. Actin-related protein 2 and actin-related protein 3 (ACTR2, ACTR3), members of the Arp2/3 complex, were the most enriched nuclear BRAF partners, and ACTR3 was highly related to lymph node stage and extrathyroidal extension. The knockdown of ACTR3, and consequently ACTR2, has a tumor suppressor effect in thyroid cells and on vemurafenib resistance. Several studies showed new roles for nuclear actin in transcriptional regulation, DNA repair, and shaping the chromatin, genomic, and epigenetic landscape [75]. Recently, Huang identified Arp2/3 complex subunits as prognostic biomarkers for hepatocellular carcinoma [76]. Further experiments are needed to explore the role of BRAF^{V600E}, ACTR2, and ACTR3 in the nucleus.

In conclusion, our findings indicate a strong relationship between nuclear BRAF^{V600E} and tumor aggressive behavior, risk of recurrence, and developing resistance against selective BRAF inhibitors. Our results demonstrate that the nuclear localization of BRAF^{V600E} is a dynamic phenomenon and may contribute to vemurafenib resistance by changing its subcellular localization according to biological demand. Such abnormal changes in the kinase localization will not only provide new insights into the mechanism of advanced tumor in PTC patients but also open new avenues for discovering novel therapeutic targets. We also present a platform for establishing a new clinical marker to identify PTC patients at high risk, so clinicians can offer them the appropriate treatment at an earlier time. The current study anticipates that early recognition and need for therapy with selective BRAF^{V600E} inhibitors will be beneficial only in patients with cytosolic BRAF^{V600E} but not with those who have BRAF^{V600E} in the nucleus. Large-scale studies are needed to confirm the correlation between the incidence of nuclear BRAF^{V600E} and poor prognosis in patients with aggressive TCs. The exact role and relevance of ACTR2, and ACTR3 with BRAF^{V600E} in the nucleus needs further studies, which will allow us to better understand the role of nuclear BRAF/ACTR complex in TC resistance.

Acknowledgements

This work was partially supported by a Pilot grant from Tulane University Health Sciences Center (E.K.), a Pilot grant from Tulane University (M.Z.), NIH/NCI R21CA194750 (Z.Y.A.), DELTA CRP Fund (Z.Y.A.) and Grant HL072889 from the NIH (AHB).

Disclosure of conflict of interest

None.

Address correspondence to: Dr. Mourad Zerfaoui, Department of Surgery, Tulane University School of Medicine, 1430 Tulane Avenue, New Orleans, LA 70112, USA. E-mail: mzerfaoui@tulane.edu

References

[1] Xing M. BRAF mutation in papillary thyroid cancer: pathogenic role, molecular bases, and clinical implications. Endocr Rev 2007; 28: 742-762.

[2] Xing M, Alzahrani AS, Carson KA, Viola D, Elisei R, Bendlova B, Yip L, Mian C, Vianello F, Tuttle RM, Robenshtok E, Fagin JA, Puxeddu E, Fugazzola L, Czarniecka A, Jarzab B, O'Neill CJ, Sywak MS, Lam AK, Riesco-Eizaguirre G, Santisteban P, Nakayama H, Tufano RP, Pai SI, Zeiger MA, Westra WH, Clark DP, Clifton-Bligh R, Sidransky D, Ladenson PW and Sykorova V. Association between BRAFV600E mutation and mortality in patients with papillary thyroid cancer. JAMA 2013; 309: 1493-1501.

[3] Zhang BH and Guan KL. Activation of B-Raf kinase requires phosphorylation of the conserved residues Thr598 and Ser601. EMBO J 2000; 19: 5429-5439.

[4] Andreadi C, Noble C, Patel B, Jin H, Aguilar Hernandez MM, Balmanno K, Cook SJ and Pritchard C. Regulation of MEK/ERK pathway

output by subcellular localization of B-Raf. Biochem Soc Trans 2012; 40: 67-72.
[5] Davies H, Bignell GR, Cox C, Stephens P, Edkins S, Clegg S, Teague J, Woffendin H, Garnett MJ, Bottomley W, Davis N, Dicks E, Ewing R, Floyd Y, Gray K, Hall S, Hawes R, Hughes J, Kosmidou V, Menzies A, Mould C, Parker A, Stevens C, Watt S, Hooper S, Wilson R, Jayatilake H, Gusterson BA, Cooper C, Shipley J, Hargrave D, Pritchard-Jones K, Maitland N, Chenevix-Trench G, Riggins GJ, Bigner DD, Palmieri G, Cossu A, Flanagan A, Nicholson A, Ho JW, Leung SY, Yuen ST, Weber BL, Seigler HF, Darrow TL, Paterson H, Marais R, Marshall CJ, Wooster R, Stratton MR and Futreal PA. Mutations of the BRAF gene in human cancer. Nature 2002; 417: 949-954.
[6] Schneider DF and Chen H. New developments in the diagnosis and treatment of thyroid cancer. CA Cancer J Clin 2013; 63: 374-394.
[7] Begum S, Rosenbaum E, Henrique R, Cohen Y, Sidransky D and Westra WH. BRAF mutations in anaplastic thyroid carcinoma: implications for tumor origin, diagnosis and treatment. Mod Pathol 2004; 17: 1359-1363.
[8] Howlader N, Noone AM, Krapcho M, Miller D, Bishop K, Altekruse SF, Kosary CL, Yu M, Ruhl J, Tatalovich Z, Mariotto A, Lewis DR, Chen HS, Feuer EJ and Cronin KA. SEER cancer statistics review, 1975-2013, National Cancer Institute. Bethesda, MD. http://seer.cancer.gov/csr/1975_2013/2016.
[9] Nikiforova MN, Kimura ET, Gandhi M, Biddinger PW, Knauf JA, Basolo F, Zhu Z, Giannini R, Salvatore G, Fusco A, Santoro M, Fagin JA and Nikiforov YE. BRAF mutations in thyroid tumors are restricted to papillary carcinomas and anaplastic or poorly differentiated carcinomas arising from papillary carcinomas. J Clin Endocrinol Metab 2003; 88: 5399-5404.
[10] Xing M, Westra WH, Tufano RP, Cohen Y, Rosenbaum E, Rhoden KJ, Carson KA, Vasko V, Larin A, Tallini G, Tolaney S, Holt EH, Hui P, Umbricht CB, Basaria S, Ewertz M, Tufaro AP, Califano JA, Ringel MD, Zeiger MA, Sidransky D and Ladenson PW. BRAF mutation predicts a poorer clinical prognosis for papillary thyroid cancer. J Clin Endocrinol Metab 2005; 90: 6373-6379.
[11] Lupi C, Giannini R, Ugolini C, Proietti A, Berti P, Minuto M, Materazzi G, Elisei R, Santoro M, Miccoli P and Basolo F. Association of BRAFV600E mutation with poor clinicopathological outcomes in 500. J Clin Endocrinol Metab 2007; 92: 4085-4090.
[12] Kim SJ, Lee KE, Myong JP, Park JH, Jeon YK, Min HS, Park SY, Jung KC, Koo do H and Youn YK. BRAFV600E mutation is associated with tumor aggressiveness in papillary thyroid. World J Surg 2012; 36: 310-317.
[13] Tang KT and Lee CH. BRAF mutation in papillary thyroid carcinoma: pathogenic role and clinical implications. J Chin Med Assoc 2010; 73: 113-128.
[14] Li C, Lee KC, Schneider EB and Zeiger MA. BRAFV600E mutation and its association with clinicopathological features of papillary thyroid cancer: a meta-analysis. J Clin Endocrinol Metab 2012; 97: 4559-4570.
[15] Li Q, Yuan J, Wang Y and Zhai Y. Association between the BRAFV600E mutation and ultrasound features of the thyroid in thyroid papillary carcinoma. Oncol Lett 2017; 14: 1439-1444.
[16] Barbaro D, Incensati RM, Materazzi G, Boni G, Grosso M, Panicucci E, Lapi P, Pasquini C and Miccoli P. The BRAFV600E mutation in papillary thyroid cancer with positive or suspected pre-surgical cytological finding is not associated with advanced stages or worse prognosis. Endocrine 2014; 45: 462-468.
[17] Fugazzola L, Mannavola D, Cirello V, Vannucchi G, Muzza M, Vicentini L and Beck-Peccoz P. BRAF mutations in an Italian cohort of thyroid cancers. Clin Endocrinol (Oxf) 2004; 61: 239-243.
[18] Niederer-Wust SM, Jochum W, Forbs D, Brandle M, Bilz S, Clerici T, Oettli R, Muller J, Haile SR, Ess S, Stoeckli SJ and Broglie MA. Impact of clinical risk scores and BRAFV600E mutation status on outcome in papillary thyroid cancer. Surgery 2015; 157: 119-125.
[19] Zoghlami A, Roussel F, Sabourin JC, Kuhn JM, Marie JP, Dehesdin D and Choussy O. BRAF mutation in papillary thyroid carcinoma: predictive value for long-term prognosis and radioiodine sensitivity. Eur Ann Otorhinolaryngol Head Neck Dis 2014; 131: 7-13.
[20] Kohno M and Pouyssegur J. Targeting the ERK signaling pathway in cancer therapy. Ann Med 2006; 38: 200-211.
[21] Liu D, Liu Z, Jiang D, Dackiw AP and Xing M. Inhibitory effects of the mitogen-activated protein kinase kinase inhibitor CI-1040 on the proliferation and tumor growth of thyroid cancer cells with BRAF or RAS mutations. J Clin Endocrinol Metab 2007; 92: 4686-4695.
[22] Liu R, Liu D, Trink E, Bojdani E, Ning G and Xing M. The Akt-specific inhibitor MK2206 selectively inhibits thyroid cancer cells harboring mutations that can activate the PI3K/Akt pathway. J Clin Endocrinol Metab 2011; 96: E577-585.
[23] Garbe C and Eigentler TK. Vemurafenib. Recent Results Cancer Res 2018; 211: 77-89.
[24] Kim KB, Cabanillas ME, Lazar AJ, Williams MD, Sanders DL, Ilagan JL, Nolop K, Lee RJ and Sherman SI. Clinical responses to vemurafenib in patients with metastatic papillary thyroid

cancer harboring BRAF (V600E) mutation. Thyroid 2013; 23: 1277-1283.
[25] Liu R, Liu D and Xing M. The Akt inhibitor MK2206 synergizes, but perifosine antagonizes, the BRAF(V600E). J Clin Endocrinol Metab 2012; 97: E173-182.
[26] Brose MS, Nutting CM, Jarzab B, Elisei R, Siena S, Bastholt L, de la Fouchardiere C, Pacini F, Paschke R, Shong YK, Sherman SI, Smit JW, Chung J, Kappeler C, Pena C, Molnar I and Schlumberger MJ. Sorafenib in radioactive iodine-refractory, locally advanced or metastatic differentiated thyroid cancer: a randomised, double-blind, phase 3 trial. Lancet 2014; 384: 319-328.
[27] Xing J, Liu R, Xing M and Trink B. The BRAFT1799A mutation confers sensitivity of thyroid cancer cells to the BRAFV600E inhibitor PLX4032 (RG7204). Biochem Biophys Res Commun 2011; 404: 958-962.
[28] Gunda V, Bucur O, Varnau J, Vanden Borre P, Bernasconi MJ, Khosravi-Far R and Parangi S. Blocks to thyroid cancer cell apoptosis can be overcome by inhibition of the MAPK and PI3K/AKT pathways. Cell Death Dis 2014; 5: e1104.
[29] Subbiah V, Kreitman RJ, Wainberg ZA, Cho JY, Schellens JHM, Soria JC, Wen PY, Zielinski C, Cabanillas ME, Urbanowitz G, Mookerjee B, Wang D, Rangwala F and Keam B. Dabrafenib and trametinib treatment in patients with locally advanced or metastatic BRAF V600-mutant anaplastic thyroid cancer. J Clin Oncol 2018; 36: 7-13.
[30] Nazarian R, Shi H, Wang Q, Kong X, Koya RC, Lee H, Chen Z, Lee MK, Attar N, Sazegar H, Chodon T, Nelson SF, McArthur G, Sosman JA, Ribas A and Lo RS. Melanomas acquire resistance to B-RAF(V600E) inhibition by RTK or N-RAS upregulation. Nature 2010; 468: 973-977.
[31] Brose MS, Cabanillas ME, Cohen EE, Wirth LJ, Riehl T, Yue H, Sherman SI and Sherman EJ. Vemurafenib in patients with BRAF(V600E)-positive metastatic or unresectable papillary thyroid cancer refractory to radioactive iodine: a non-randomised, multicentre, open-label, phase 2 trial. Lancet Oncol 2016; 17: 1272-1282.
[32] Crispo F, Notarangelo T, Pietrafesa M, Lettini G, Storto G, Sgambato A, Maddalena F and Landriscina M. BRAF inhibitors in thyroid cancer: clinical impact, mechanisms of resistance and future perspectives. Cancers (Basel) 2019; 11: 1388.
[33] Proietti I, Skroza N, Bernardini N, Tolino E, Balduzzi V, Marchesiello A, Michelini S, Volpe S, Mambrin A, Mangino G, Romeo G, Maddalena P, Rees C and Potenza C. Mechanisms of acquired BRAF inhibitor resistance in melanoma: a systematic review. Cancers (Basel) 2020; 12: 2801.
[34] Li QS, Shen BN, Xu HJ and Ruan BF. Promising strategies for overcoming BRAF inhibitor resistance based on known resistance mechanisms. Anticancer Agents Med Chem 2020; 20: 1415-1430.
[35] Tangella LP, Clark ME and Gray ES. Resistance mechanisms to targeted therapy in BRAF-mutant melanoma - a mini review. Biochim Biophys Acta Gen Subj 2021; 1865: 129736.
[36] Subbiah V, Baik C and Kirkwood JM. Clinical development of BRAF plus MEK inhibitor combinations. Trends Cancer 2020; 6: 797-810.
[37] Chapman PB, Hauschild A, Robert C, Haanen JB, Ascierto P, Larkin J, Dummer R, Garbe C, Testori A, Maio M, Hogg D, Lorigan P, Lebbe C, Jouary T, Schadendorf D, Ribas A, O'Day SJ, Sosman JA, Kirkwood JM, Eggermont AM, Dreno B, Nolop K, Li J, Nelson B, Hou J, Lee RJ, Flaherty KT and McArthur GA. Improved survival with vemurafenib in melanoma with BRAFV600E mutation. N Engl J Med 2011; 364: 2507-2516.
[38] Hauschild A, Grob JJ, Demidov LV, Jouary T, Gutzmer R, Millward M, Rutkowski P, Blank CU, Miller WH Jr, Kaempgen E, Martin-Algarra S, Karaszewska B, Mauch C, Chiarion-Sileni V, Martin AM, Swann S, Haney P, Mirakhur B, Guckert ME, Goodman V and Chapman PB. Dabrafenib in BRAF-mutated metastatic melanoma: a multicentre, open-label, phase 3 randomised controlled trial. Lancet 2012; 380: 358-365.
[39] Lemoine NR, Mayall ES, Jones T, Sheer D, McDermid S, Kendall-Taylor P and Wynford-Thomas D. Characterisation of human thyroid epithelial cells immortalised in vitro by simian virus 40 DNA transfection. Br J Cancer 1989; 60: 897-903.
[40] Galabova-Kovacs G, Matzen D, Piazzolla D, Meissl K, Plyushch T, Chen AP, Silva A and Baccarini M. Essential role of B-Raf in ERK activation during extraembryonic development. Proc Natl Acad Sci U S A 2006; 103: 1325-1330.
[41] Tsumagari K, Abd Elmageed ZY, Sholl AB, Friedlander P, Abdraboh M, Xing M, Boulares AH and Kandil E. Simultaneous suppression of the MAP kinase and NF-kappaB pathways provides a robust therapeutic potential for thyroid cancer. Cancer Lett 2015; 368: 46-53.
[42] Antonello ZA and Nucera C. Orthotopic mouse models for the preclinical and translational study of targeted therapies against metastatic human thyroid carcinoma with BRAF (V600E) or wild-type BRAF. Oncogene 2014; 33: 5397-5404.
[43] Lito P, Pratilas CA, Joseph EW, Tadi M, Halilovic E, Zubrowski M, Huang A, Wong WL, Callahan

MK, Merghoub T, Wolchok JD, de Stanchina E, Chandarlapaty S, Poulikakos PI, Fagin JA and Rosen N. Relief of profound feedback inhibition of mitogenic signaling by RAF inhibitors attenuates their activity in BRAFV600E melanomas. Cancer Cell 2013; 22: 668-682.

[44] Heier CR and DiDonato CJ. Translational readthrough by the aminoglycoside geneticin (G418) modulates SMN stability in vitro and improves motor function in SMA mice in vivo. Hum Mol Genet 2009; 18: 1310-1322.

[45] Kandil E, Hauch A, Friedlander P, Sheng M, Tsumagari K, Saeed A, Gimble JM and Rowan BG. A novel mouse model of metastatic thyroid carcinoma using human adipose tissue-derived stromal/stem cells. Anticancer Res 2013; 33: 4213-4217.

[46] Abd Elmageed ZY, Sholl AB, Tsumagari K, Al-Qurayshi Z, Basolo F, Moroz K, Boulares H, Friedlander F, Miccoli P and Kandil E. Immunohistochemistry as an accurate tool for evaluating BRAF-V600E mutation in 130 samples of papillary thyroid cancer. Surgery 2017; 161: 1122-1128.

[47] Dvorak K, Aggeler B, Palting J, McKelvie P, Ruszkiewicz A and Waring P. Immunohistochemistry with the anti-BRAFV600E (VE1) antibody: impact of pre-analytical conditions and concordance with DNA sequencing in colorectal and papillary thyroid carcinoma. Pathology 2014; 46: 509-517.

[48] Abd Elmageed ZY, Sholl AB, Tsumagari K, Al-Qurayshi Z, Basolo F, Moroz K, Boulares AH, Friedlander P, Miccoli P and Kandil E. Immunohistochemistry as an accurate tool for evaluating BRAF-V600E mutation in 130 samples of papillary thyroid cancer. Surgery 2017; 161: 1122-1128.

[49] Tyanova S, Temu T and Cox J. The MaxQuant computational platform for mass spectrometry-based shotgun proteomics. Nat Protoc 2016; 11: 2301-2319.

[50] Soudy M, Anwar AM, Ahmed EA, Osama A, Ezzeldin S, Mahgoub S and Magdeldin S. UniprotR: retrieving and visualizing protein sequence and functional information from Universal Protein Resource (UniProt knowledgebase). J Proteomics 2020; 213: 103613.

[51] Routhier CA, Mochel MC, Lynch K, Dias-Santagata D, Louis DN and Hoang MP. Comparison of 2 monoclonal antibodies for immunohistochemical detection of BRAFV600E mutation in malignant melanoma, pulmonary carcinoma, gastrointestinal carcinoma, thyroid carcinoma, and gliomas. Hum Pathol 2013; 44: 2563-2570.

[52] Zhao M, Sano D, Pickering CR, Jasser SA, Henderson YC, Clayman GL, Sturgis EM, Ow TJ, Lotan R, Carey TE, Sacks PG, Grandis JR, Sidransky D, Heldin NE and Myers JN. Assembly and initial characterization of a panel of 85 genomically validated cell lines from diverse head and neck tumor sites. Clin Cancer Res 2011; 17: 7248-7264.

[53] Patel H, Mishra R, Yacoub N, Alanazi S, Kilroy MK and Garrett JT. IGF1R/IR mediates resistance to BRAF and MEK inhibitors in BRAF-mutant melanoma. Cancers (Basel) 2021; 13: 5863.

[54] Dai X, Zhang X, Yin Q, Hu J, Guo J, Gao Y, Snell AH, Inuzuka H, Wan L and Wei W. Acetylation-dependent regulation of BRAF oncogenic function. Cell Rep 2022; 38: 110250.

[55] Kau TR, Way JC and Silver PA. Nuclear transport and cancer: from mechanism to intervention. Nat Rev Cancer 2004; 4: 106-117.

[56] Zerfaoui M, Dokunmu TM, Toraih EA, Rezk BM, Abd Elmageed ZY and Kandil E. New insights into the link between melanoma and thyroid cancer: role of nucleocytoplasmic trafficking. Cells 2021; 10: 367.

[57] Wagstaff KM, Sivakumaran H, Heaton SM, Harrich D and Jans DA. Ivermectin is a specific inhibitor of importin alpha/beta-mediated nuclear import able to inhibit replication of HIV-1 and dengue virus. Biochem J 2012; 443: 851-856.

[58] Hu J, Stites EC, Yu H, Germino EA, Meharena HS, Stork PJ, Kornev AP, Taylor SS and Shaw AS. Allosteric activation of functionally asymmetric RAF kinase dimers. Cell 2013; 154: 1036-1046.

[59] Bollag G, Hirth P, Tsai J, Zhang J, Ibrahim PN, Cho H, Spevak W, Zhang C, Zhang Y, Habets G, Burton EA, Wong B, Tsang G, West BL, Powell B, Shellooe R, Marimuthu A, Nguyen H, Zhang KY, Artis DR, Schlessinger J, Su F, Higgins B, Iyer R, D'Andrea K, Koehler A, Stumm M, Lin PS, Lee RJ, Grippo J, Puzanov I, Kim KB, Ribas A, McArthur GA, Sosman JA, Chapman PB, Flaherty KT, Xu X, Nathanson KL and Nolop K. Clinical efficacy of a RAF inhibitor needs broad target blockade in BRAF-mutant melanoma. Nature 2010; 467: 596-599.

[60] Day F, Muranyi A, Singh S, Shanmugam K, Williams D, Byrne D, Pham K, Palmieri M, Tie J, Grogan T, Gibbs P, Sieber O, Waring P and Desai J. A mutant BRAFV600E-specific immunohistochemical assay: correlation with molecular mutation status and clinical outcome in colorectal cancer. Target Oncol 2015; 10: 99-109.

[61] Capper D, Preusser M, Habel A, Sahm F, Ackermann U, Schindler G, Pusch S, Mechtersheimer G, Zentgraf H and von Deimling A. Assessment of BRAFV600E mutation status by immunohistochemistry with a mutation-specific monoclonal antibody. Acta Neuropathol 2011; 122: 11-19.

[62] Abd Elmageed ZY, Moore RF, Tsumagari K, Lee MM, Sholl AB, Friedlander P, Al-Qurayshi Z, Hassan M, Wang AR, Boulares HA and Kandil E. Prognostic role of BRAF(V600E) cellular localization in melanoma. J Am Coll Surg 2018; 226: 526-537.

[63] Salas Fragomeni RA, Chung HW, Landesman Y, Senapedis W, Saint-Martin JR, Tsao H, Flaherty KT, Shacham S, Kauffman M and Cusack JC. CRM1 and BRAF inhibition synergize and induce tumor regression in BRAF-mutant melanoma. Mol Cancer Ther 2013; 12: 1171-1179.

[64] Plotnikov A, Zehorai E, Procaccia S and Seger R. The MAPK cascades: signaling components, nuclear roles and mechanisms of nuclear translocation. Biochim Biophys Acta 2011; 1813: 1619-1633.

[65] Terry LJ, Shows EB and Wente SR. Crossing the nuclear envelope: hierarchical regulation of nucleocytoplasmic transport. Science 2007; 318: 1412-1416.

[66] Hill R, Cautain B, de Pedro N and Link W. Targeting nucleocytoplasmic transport in cancer therapy. Oncotarget 2014; 5: 11-28.

[67] Anwar MA, Murad F, Dawson E, Abd Elmageed ZY, Tsumagari K and Kandil E. Immunohistochemistry as a reliable method for detection of BRAF-V600E mutation in melanoma: a systematic review and meta-analysis of current published literature. J Surg Res 2016; 203: 407-415.

[68] Lo MC, Paterson A, Maraka J, Clark R, Goodwill J, Nobes J, Garioch J, Moncrieff M, Rytina E and Igali L. A UK feasibility and validation study of the VE1 monoclonal antibody immunohistochemistry stain for BRAF-V600E mutations in metastatic melanoma. Br J Cancer 2016; 115: 223-7.

[69] Long GV, Wilmott JS, Capper D, Preusser M, Zhang YE, Thompson JF, Kefford RF, von Deimling A and Scolyer RA. Immunohistochemistry is highly sensitive and specific for the detection of V600E BRAF mutation in melanoma. Am J Surg Pathol 2013; 37: 61-65.

[70] Schafroth C, Galvan JA, Centeno I, Koelzer VH, Dawson HE, Sokol L, Rieger G, Berger MD, Hadrich M, Rosenberg R, Nitsche U, Schnuriger B, Langer R, Inderbitzin D, Lugli A and Zlobec I. VE1 immunohistochemistry predicts BRAFV600E mutation status and clinical outcome in colorectal cancer. Oncotarget 2015; 6: 41453-41463.

[71] Moriceau G, Hugo W, Hong A, Shi H, Kong X, Yu CC, Koya RC, Samatar AA, Khanlou N, Braun J, Ruchalski K, Seifert H, Larkin J, Dahlman KB, Johnson DB, Algazi A, Sosman JA, Ribas A and Lo RS. Tunable-combinatorial mechanisms of acquired resistance limit the efficacy of BRAF/MEK cotargeting but result in melanoma drug addiction. Cancer Cell 2015; 27: 240-256.

[72] Antonello ZA, Hsu N, Bhasin M, Roti G, Joshi M, Van Hummelen P, Ye E, Lo AS, Karumanchi SA, Bryke CR and Nucera C. Vemurafenib-resistance via de novo RBM genes mutations and chromosome 5 aberrations is overcome by combined therapy with palbociclib in thyroid carcinoma with BRAF(V600E). Oncotarget 2017; 8: 84743-84760.

[73] Shi X, Liu R, Basolo F, Giannini R, Shen X, Teng D, Guan H, Shan Z, Teng W, Musholt TJ, Al-Kuraya K, Fugazzola L, Colombo C, Kebebew E, Jarzab B, Czarniecka A, Bendlova B, Sykorova V, Sobrinho-Simoes M, Soares P, Shong YK, Kim TY, Cheng S, Asa SL, Viola D, Elisei R, Yip L, Mian C, Vianello F, Wang Y, Zhao S, Oler G, Cerutti JM, Puxeddu E, Qu S, Wei Q, Xu H, O'Neill CJ, Sywak MS, Clifton-Bligh R, Lam AK, Riesco-Eizaguirre G, Santisteban P, Yu H, Tallini G, Holt EH, Vasko V and Xing M. Differential clinicopathological risk and prognosis of major papillary thyroid cancer variants. J Clin Endocrinol Metab 2016; 101: 264-274.

[74] Huang Y, Qu S, Zhu G, Wang F, Liu R, Shen X, Viola D, Elisei R, Puxeddu E, Fugazzola L, Colombo C, Jarzab B, Czarniecka A, Lam AK, Mian C, Vianello F, Yip L, Riesco-Eizaguirre G, Santisteban P, O'Neill CJ, Xing M, Sywak MS, Clifton-Bligh R, Bendlova B and Sykorova V. BRAFV600E mutation-assisted risk stratification of solitary intrathyroidal papillary thyroid cancer for precision treatment. J Natl Cancer Inst 2018; 110: 362-370.

[75] Kloc M, Chanana P, Vaughn N, Uosef A, Kubiak JZ and Ghobrial RM. New insights into cellular functions of nuclear actin. Biology (Basel) 2021; 10: 304.

[76] Huang S, Li D, Zhuang L, Sun L and Wu J. Identification of Arp2/3 complex subunits as prognostic biomarkers for hepatocellular carcinoma. Front Mol Biosci 2021; 8: 690151.

Supplementary Table 1. List of cell lines and their BRAF and N-RAS status used in this study

	Origin	Cell line	BRAF status	NRAS status	Reference
1	Thyroid Cancer	K1	V600E	WT	Xing et al. [1]
2		KAT18	WT	WT	
3		NPA	V600E	WT	
4		TPC1	WT	WT	
5		SW1736	V600E	WT	Xing et al. [1, 2]
6		MDA-T32	V600E	WT	Henderson [3]
7	Thyroid Cancer	BCPAP	V600E	WT	Schweppe [4]
8	Normal Thyroid	Nthy-Ori-3-1	WT	WT	Lemoine [5]
9	Fibroblasts	MEF-BRAF$^{-/-}$	Knockout	WT	Baccarini [6]

References

[1] Xing J, Liu R, Xing M and Trink B. The BRAFT1799A mutation confers sensitivity of thyroid cancer cells to the BRAFV600E inhibitor PLX4032 (RG7204). Biochem Biophys Res Commun 2011; 404: 958-962.

[2] Gunda V, Bucur O, Varnau J, Vanden Borre P, Bernasconi MJ, Khosravi-Far R and Parangi S. Blocks to thyroid cancer cell apoptosis can be overcome by inhibition of the MAPK and PI3K/AKT pathways. Cell Death Dis 2014; 5: e1104.

[3] Henderson YC, Ahn SH, Ryu J, Chen Y, Williams MD, El-Naggar AK, Gagea M, Schweppe RE, Haugen BR, Lai SY and Clayman GL. Development and characterization of six new human papillary thyroid carcinoma cell lines. J Clin Endocrinol Metab 2015; 100: E243-252.

[4] Schweppe RE, Klopper JP, Korch C, Pugazhenthi U, Benezra M, Knauf JA, Fagin JA, Marlow LA, Copland JA, Smallridge RC and Haugen BR. Deoxyribonucleic acid profiling analysis of 40 human thyroid cancer cell lines reveals cross-contamination resulting in cell line redundancy and misidentification. J Clin Endocrinol Metab 2008; 93: 4331-4341.

[5] Lemoine NR, Mayall ES, Jones T, Sheer D, McDermid S, Kendall-Taylor P and Wynford-Thomas D. Characterisation of human thyroid epithelial cells immortalised in vitro by simian virus 40 DNA transfection. Br J Cancer 1989; 60: 897-903.

[6] Galabova-Kovacs G, Matzen D, Piazzolla D, Meissl K, Plyushch T, Chen AP, Silva A and Baccarini M. Essential role of B-Raf in ERK activation during extraembryonic development. Proc Natl Acad Sci U S A 2006; 103: 1325-1330.